Transp Porous Med
DOI 10.1007/s11242-010-9601-0

Non-similar Solution for Natural Convective Boundary Layer Flow Over a Sphere Embedded in a Porous Medium Saturated with a Nanofluid

Ali Chamkha · Rama Subba Reddy Gorla · Kaustubh Ghodeswar

Received: 14 May 2010 / Accepted: 31 May 2010

Abstract A boundary layer analysis is presented for the natural convection past an isothermal sphere in a Darcy porous medium saturated with a nanofluid. Numerical results for friction factor, surface heat transfer rate, and mass transfer rate have been presented for parametric variations of the buoyancy ratio parameter N_r, Brownian motion parameter N_b, thermophoresis parameter N_t, and Lewis number L_e. The dependency of the friction factor, surface heat transfer rate (Nusselt number), and mass transfer rate (Sherwood number) on these parameters has been discussed.

Keywords Natural convection · Porous medium · Nanofluid

List of Symbols

D_B Brownian diffusion coefficient
D_T Thermophoretic diffusion coefficient
f Rescaled nano-particle volume fraction
g Gravitational acceleration vector
k_m Effective thermal conductivity of the porous medium
K Permeability of porous medium
L_e Lewis number
N_r Buoyancy Ratio
N_b Brownian motion parameter
N_t Thermophoresis parameter
Nu Nusselt number

A. Chamkha
Public Authority for Applied Education and Training, Shuweikh, Kuwait
e-mail: achamkha@yahoo.com

R. S. R. Gorla (✉) · K. Ghodeswar
Cleveland State University, Cleveland, OH 44115, USA
e-mail: r.gorla@csuohio.edu

Published online: 19 June 2010

P	Pressure
q''	Wall heat flux
Ra_x	Local Rayleigh number
S	Dimensionless stream function
T	Temperature
T_W	Wall temperature at vertical cone
T_∞	Ambient temperature attained as y tends to infinity
U	Reference velocity
Pr	Prandtl number
Re	Reynolds number
u, v	Darcy velocity components
(x, y)	Cartesian coordinates

Greek Symbols

α_m	Thermal diffusivity of porous medium
β	Volumetric expansion coefficient of fluid
ε	Porosity
η	Dimensionless distance
θ	Dimensionless temperature
μ	Viscosity of fluid
ρ_f	Fluid density
ρ_p	Nano-particle mass density
$(\rho c)_f$	Heat capacity of the fluid
$(\rho c)_m$	Effective heat capacity of porous medium
$(\rho c)_p$	Effective heat capacity of nano-particle material
τ	Parameter defined by Eq. 5
ϕ	Nano-particle volume fraction
ϕ_W	Nano-particle volume fraction at vertical cone
ϕ_∞	Ambient nano-particle volume fraction attained
ψ	Stream function

1 Introduction

Porous media heat transfer problems have several engineering applications such as geothermal energy recovery, crude oil extraction, ground water pollution, thermal energy storage, and flow through filtering media. Cheng and Minkowycz (1977) presented similarity solutions for free convective heat transfer from a vertical plate in a fluid-saturated porous medium. The problem of combined convection from vertical plates in porous media was studied by Minkowycz et al. (1985) and Ranganathan and Viskanta (1984). All these studies were concerned with Newtonian fluid flows. The boundary layer flows in nanofluids have been analyzed recently by Nield and Kuznetsov (2009a,b). A clear picture about the nanofluid boundary layer flows is still to emerge.

Similarity solutions for free convection from a sphere embedded in a porous medium at high Raleigh numbers was presented by Cheng (1985). This was a special case of the natural convection about a general axisymmetric body embedded in a porous medium considered by Merkin (1979). Conjugate steady convection from a solid sphere with an isothermal heated core was investigated by Kimura and Pop (1994). Sano (1996) studied the unsteady forced and natural convection around a sphere immersed in a fluid-saturated porous medium. He used the method of asymptotic expansions to obtain a solution for the energy equation. Buoyancy driven thermal free convection from a sphere in a porous medium was studied analytically by Ganapathy (1997). He obtained series solutions in terms of Rayleigh number (Ra). Yan et al. (1997) presented numerical solutions for the transient problem corresponding to step changes in surface temperature or heat flux of the sphere. Pop and Ingham (1990) presented a second order boundary layer theory for large Ra and used a finite difference scheme to obtain numerical results for finite values of Ra.

This study has been undertaken to analyze the natural convection past a sphere embedded in a non-Darcy porous medium saturated by a nanofluid. The effects of Brownian motion and thermophoresis are included for the nanofluid. Numerical solutions of the boundary layer equations are obtained, and discussion is provided for several values of the nanofluid parameters governing the problem.

2 Analysis

We consider the steady free convection boundary layer flow past a sphere placed in a nanofluid saturated porous medium. The co-ordinate system is selected such that x measures the distance along the surface of the sphere from the stagnation point and y measures the distance normal to the surface of the sphere. The radius of sphere is a (Fig. 1).

At $y = 0$, the temperature T and the nano-particle fraction ϕ take constant values T_W and ϕ_W, respectively. The ambient values, attend as y tends to infinity, of T and ϕ are denoted by T_∞ and ϕ_∞, respectively. The Oberbeck-Boussinesq approximation is employed. Homogeneity and local thermal equilibrium in the porous medium are assumed. We consider the porous medium whose porosity is denoted by ε and permeability by K.

We now make the standard boundary layer approximation based on a scale analysis and write the governing equations:

$$\frac{\partial}{\partial x}(ru) + \frac{\partial}{\partial y}(rv) = 0 \tag{1}$$

$$\frac{\partial u}{\partial y} = \frac{(1-\phi_\infty)\,\rho_{f\infty}\beta g K \sin(x/a)}{\mu}\cdot\frac{\partial T}{\partial y} - \frac{(\rho_p - \rho_{f\infty})\,gK\sin(x/a)}{\mu}\cdot\frac{\partial \phi}{\partial y} \tag{2}$$

$$u\cdot\frac{\partial T}{\partial x} + v\cdot\frac{\partial T}{\partial y} = \alpha_m\frac{\partial^2 T}{\partial y^2} + \tau\left[D_B\frac{\partial \phi}{\partial y}\frac{\partial T}{\partial y} + \frac{D_T}{T_\infty}\left(\frac{\partial T}{\partial y}\right)^2\right] \tag{3}$$

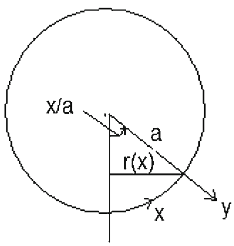

Fig. 1 Flow model and coordinate system

$$\frac{1}{\varepsilon}\left(u\frac{\partial\phi}{\partial x}+v\frac{\partial\phi}{\partial y}\right)=D_{\mathrm{B}}\frac{\partial^2\phi}{\partial y^2}+\left(\frac{D_{\mathrm{T}}}{T_\infty}\right)\frac{\partial^2 T}{\partial y^2} \tag{4}$$

where

$$\alpha_{\mathrm{m}}=\frac{k_{\mathrm{m}}}{(\rho c)_{\mathrm{f}}},\qquad \tau=\frac{\varepsilon\,(\rho c)_{\mathrm{p}}}{(\rho c)_{\mathrm{f}}} \tag{5}$$

The boundary conditions are taken to be

$$v=0,\quad T=T_{\mathrm{W}},\quad \phi=\phi_{\mathrm{W}},\qquad \text{at}\quad y=0, \tag{6}$$

$$u=v=0,\quad T\to T_\infty,\quad \phi\to\phi_\infty,\qquad \text{as}\quad y\to\infty \tag{7}$$

We introduce a stream line function ψ defined by

$$u=\frac{1}{r}\frac{\partial\psi}{\partial y},\qquad v=-\frac{1}{r}\frac{\partial\psi}{\partial x} \tag{8}$$

so that Eq. 1 is satisfied identically. We are then left with the following three equations.

$$\frac{1}{r}\frac{\partial^2\psi}{\partial y^2}=\frac{(1-\phi_\infty)\,\rho_{\mathrm{f}\infty}\beta g K\sin(x/a)}{\mu}\frac{\partial T}{\partial y}-\frac{\left(\rho_{\mathrm{p}}-\rho_{\mathrm{f}\infty}\right)gK\sin(x/a)}{\mu}\frac{\partial\phi}{\partial y} \tag{9}$$

$$\frac{1}{r}\frac{\partial\psi}{\partial y}\frac{\partial T}{\partial x}-\frac{1}{r}\frac{\partial\psi}{\partial x}\frac{\partial T}{\partial y}=\alpha_{\mathrm{m}}\frac{\partial^2 T}{\partial y^2}+\tau\left[D_{\mathrm{B}}\frac{\partial\phi}{\partial y}\frac{\partial T}{\partial y}+\left(\frac{D_{\mathrm{T}}}{T_\infty}\right)\left(\frac{\partial T}{\partial y}\right)^2\right] \tag{10}$$

$$\frac{1}{\varepsilon}\left(\frac{1}{r}\frac{\partial\psi}{\partial y}\frac{\partial\phi}{\partial x}-\frac{1}{r}\frac{\partial\psi}{\partial x}\frac{\partial\phi}{\partial y}\right)=D_{\mathrm{B}}\frac{\partial^2\phi}{\partial y^2}+\left(\frac{D_{\mathrm{T}}}{T_\infty}\right)\frac{\partial^2 T}{\partial y^2} \tag{11}$$

Proceeding with the analysis, we introduce the following dimensionless variables:

$$\begin{aligned}
\eta&=\frac{y}{x}\cdot Ra_x^{1/2}\\
\xi&=x/a\\
r&=a\cdot\sin(x/a)\\
Ra_x&=\frac{(1-\phi_\infty)\,\rho_{\mathrm{f}\infty}\beta g K x\,(T_{\mathrm{W}}-T_\infty)}{\mu\cdot\alpha_{\mathrm{m}}}\\
S&=\frac{\psi}{\alpha_{\mathrm{m}}\cdot r\cdot Ra_x^{1/2}}\\
\theta&=\frac{T-T_\infty}{T_{\mathrm{W}}-T_\infty}\\
f&=\frac{\phi-\phi_\infty}{\phi_{\mathrm{W}}-\phi_\infty}
\end{aligned} \tag{12}$$

Substituting the expressions in Eq. 12 into the governing Eqs. 9–11, we obtain the following transformed equations:

$$S''-\sin\xi\left(\theta'+N_{\mathrm{r}}\cdot f'\right)=0 \tag{13}$$

$$\theta''+\frac{1}{2}\theta'+N_{\mathrm{b}}\cdot f'\cdot\theta'+N_{\mathrm{t}}\left(\theta'\right)^2=\xi\left\{S'\frac{\partial\theta}{\partial\xi}-\theta'\left(\cot\xi+\frac{\partial S}{\partial\xi}\right)\right\} \tag{14}$$

$$f''+\frac{1}{2}L_{\mathrm{e}}\cdot f'+\frac{N_{\mathrm{t}}}{N_{\mathrm{b}}}\theta''=L_{\mathrm{e}}\cdot\xi\left\{S'\frac{\partial f}{\partial\xi}-f'\left(\cot\xi+\xi\cdot\frac{\partial S}{\partial\xi}\right)\right\} \tag{15}$$

where the parameters are defined as

$$N_r = \frac{\left(\rho_p - \rho_{f\infty}\right)\left(\phi_W - \phi_\infty\right)}{\rho_{f\infty}\beta\left(T_W - T_\infty\right)\left(1 - \phi_\infty\right)},$$
$$N_b = \frac{\varepsilon\left(\rho c\right)_p D_B\left(\phi_W - \phi_\infty\right)}{\left(\rho c\right)_f \alpha_m},$$
$$N_t = \frac{\varepsilon\left(\rho c\right)_p D_T\left(T_W - T_\infty\right)}{\left(\rho c\right)_f \alpha_m T_\infty},$$
$$L_e = \frac{\alpha_m}{\varepsilon \cdot D_B},$$
$$Pr = \frac{\mu}{\rho \cdot \alpha_m} \tag{16}$$

The transformed boundary conditions are

$$\eta = 0: \quad S = 0, \quad \theta = 1, \quad f = 1$$
$$\eta \to \infty: \quad S' = 0, \quad \theta = 0, \quad f = 0 \tag{17}$$

The heat transfer rate is given by

$$q_W = -k_f \left.\frac{\partial T}{\partial y}\right)_{y=0}$$

The heat transfer coefficient is given by

$$h = \frac{q_W}{\left(T_W - T_\infty\right)}$$

Local Nusselt number is given by

$$Nu_x = \frac{h \cdot x}{k_f} = -Ra_x^{\frac{1}{2}} \cdot \theta'\left(\xi, 0\right) \tag{18}$$

The mass transfer rate is given by

$$N_W = -D \left.\frac{\partial \phi}{\partial y}\right)_{y=0} = h_m\left(\phi_W - \phi_\infty\right)$$

where h_m = mass transfer coefficient,

$$N_W = -D \cdot \left(\phi_W - \phi_\infty\right) f' \cdot \frac{Ra_x^{1/2}}{x}$$

Sherwood number is given by

$$Sh = \frac{h_m \cdot x}{D} = -Ra_x^{\frac{1}{2}} \cdot f'\left(\xi, 0\right) \tag{19}$$

The local friction factor is given by Cf_x:

$$\tau_W = \mu \cdot \left.\frac{\partial u}{\partial y}\right)_{y=0}$$

$$Cf_x = \frac{\tau_W}{\left(\frac{\rho U^2}{2}\right)} = \frac{2 \cdot Ra_x^{\frac{3}{2}} \cdot S''\left(\xi, 0\right)}{Re_x^2 \cdot Pr} \tag{20}$$

3 Results and Discussion

Equations 13–15 were solved numerically to satisfy the boundary conditions (17) for the parametric values of L_e, N_r (buoyancy ratio number), N_b (Brownian motion parameter), and N_t (thermophoresis parameter) using finite difference method.

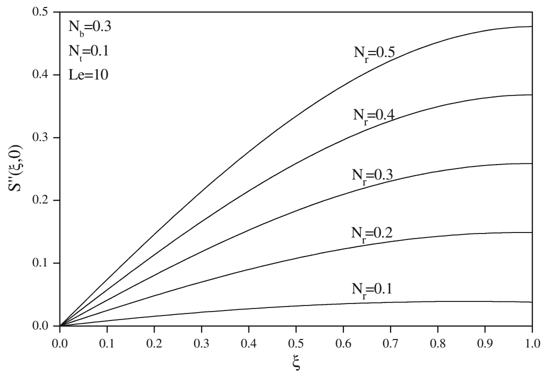

Fig. 2 Effects of N_r on skin-friction coefficient

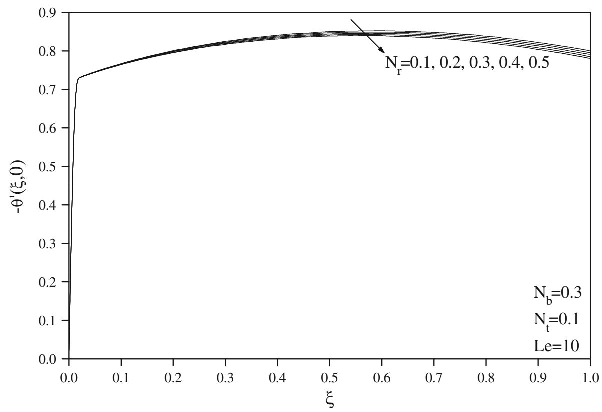

Fig. 3 Effects of N_r on heat transfer rate

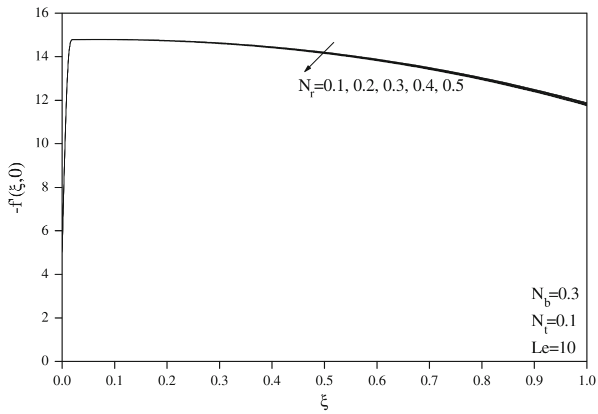

Fig. 4 Effects of N_r on mass transfer rate

Figures 2–4 indicate that as N_r increases, heat transfer rate (Nusselt number) and mass transfer rate (Sherwood number) decrease and the skin-friction coefficient increases. The temperature and concentration distributions are not influenced by N_r.

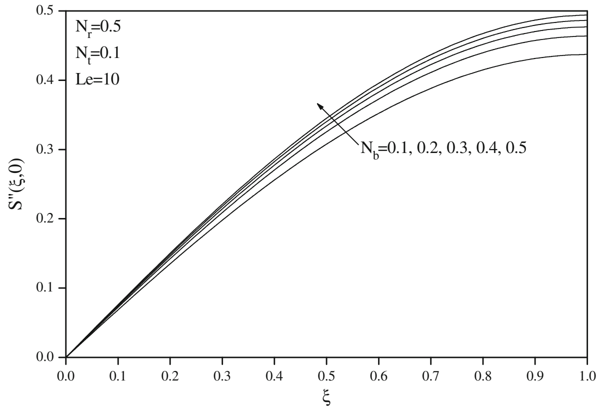

Fig. 5 Effects of N_b on skin-friction coefficient

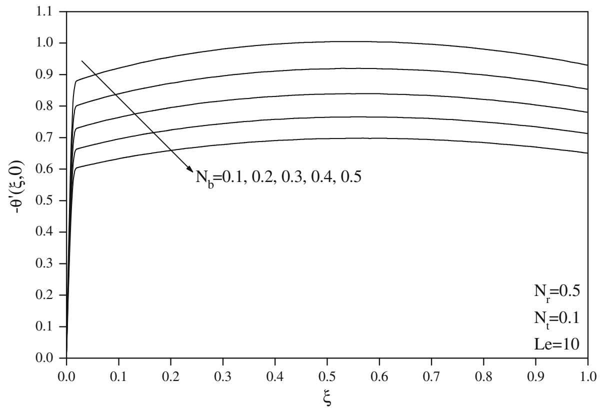

Fig. 6 Effects of N_b on heat transfer rate

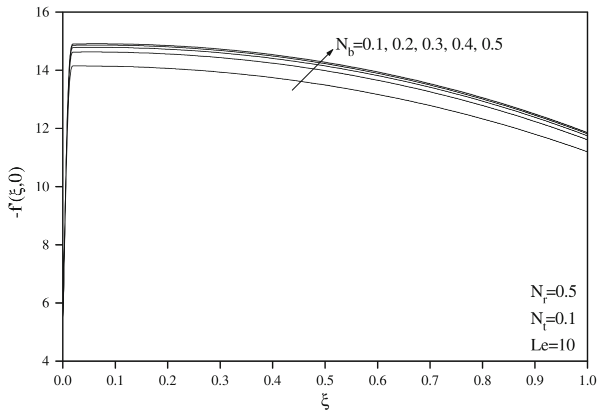

Fig. 7 Effects of N_b on mass transfer rate

Figures 5–7 indicate that as N_b increases, mass transfer rate (Sherwood number) and the skin-friction coefficient increase whereas heat transfer rate (Nusselt number) decreases.

Figures 8–10 indicate that as N_t increases, heat transfer rate (Nusselt number), mass transfer rate (Sherwood number), and the skin-friction coefficient decrease.

Fig. 8 Effects of N_t on skin-friction coefficient

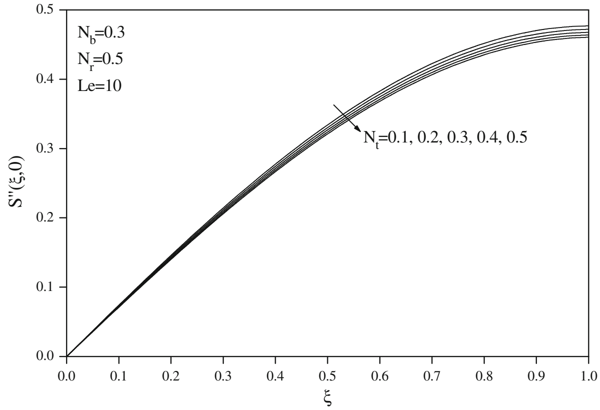

Fig. 9 Effects of N_t on heat transfer rate

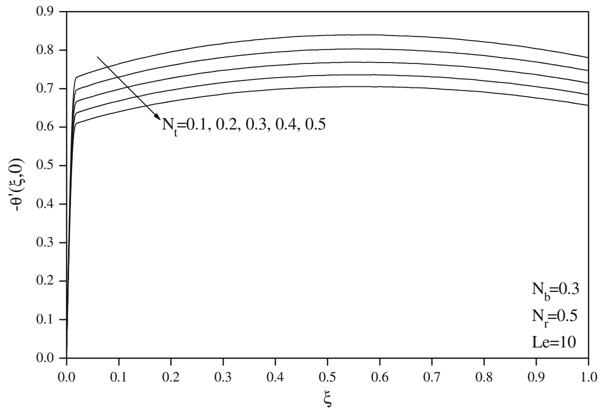

Fig. 10 Effects of N_t on mass transfer rate

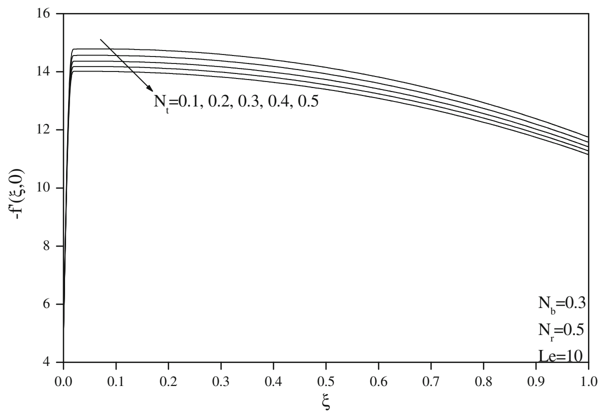

Fig. 11 Effects of L_e on skin-friction coefficient

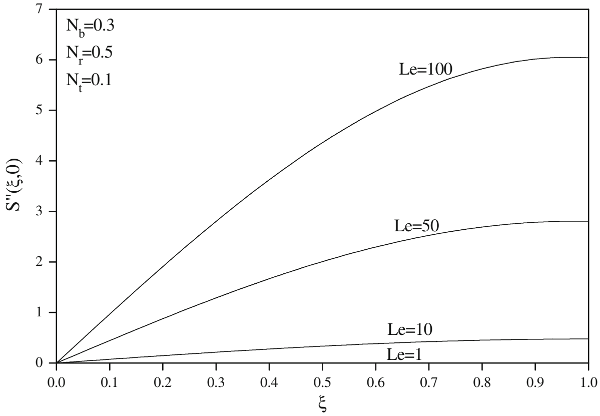

Fig. 12 Effects of L_e on heat transfer rate

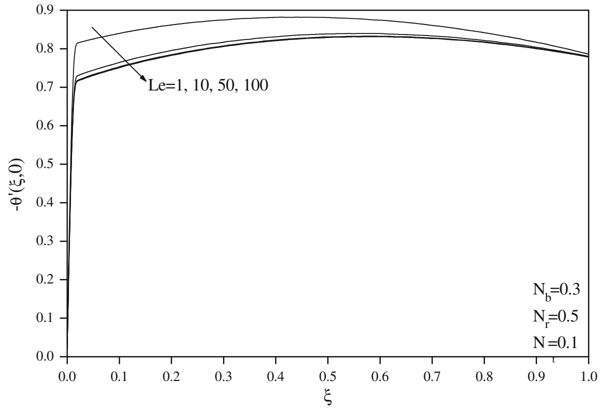

Fig. 13 Effects of L_e on mass transfer rate

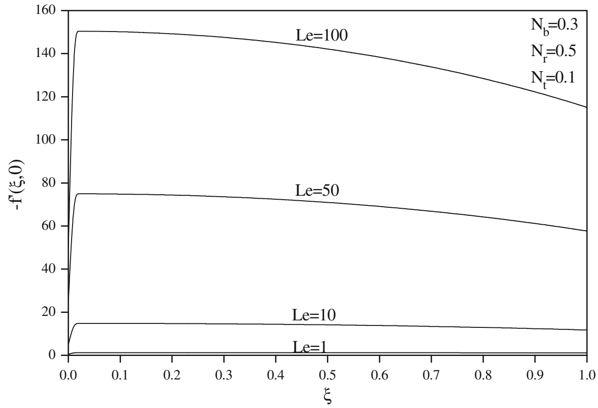

Figures 11–13 indicate that as L_e increases, the skin-friction coefficient and mass transfer rate (Sherwood number) within the boundary layer increase whereas temperature, concentration, and heat transfer rate (Nusselt number) within the boundary layer decrease.

4 Concluding Remarks

In this article, we presented a boundary layer analysis for the natural convection past a sphere embedded in a porous medium saturated with a nanofluid. Numerical results for friction factor, surface heat transfer rate, and mass transfer rate have been presented for parametric variations of the buoyancy ratio parameter N_{r}, Brownian motion parameter N_{b}, thermophoresis parameter N_{t}, and Lewis number L_{e}. The results indicate that as N_{r} and N_{t} increase, the friction factor increases, whereas the heat transfer rate (Nusselt number) and mass transfer rate (Sherwood number) decrease. As N_{b} increases, the friction factor and surface mass transfer rates increase, whereas the surface heat transfer rate decreases. As L_{e} increases, the heat and mass transfer rates increase.

References

Cheng, P.: Natural Convection in a Porous Medium: Natural Convection: Fundamentals and Applications, pp. 475–513. Hemisphere Publishers, Washington, DC (1985)

Cheng, P., Minkowycz, W.J.: Free convection about a vertical flat plate embedded in a saturated porous medium with applications to heat transfer from a dike. J. Geophys. Res. **82**, 2040–2044 (1977)

Ganapathy, R.: Time dependent free convection motion and heat transfer in an infinite porous medium induced by a heated sphere. Int. J. Heat Mass Transf. **40**, 1551–1557 (1997)

Kimura, S., Pop, I.: Conjugate free convection from a sphere in a porous medium. Int. J. Heat Mass Transf. **37**, 2187–2192 (1994)

Merkin, J.H.: Free convection boundary layers on axisymmetric and two dimensional bodies of arbitrary shape in a saturated porous medium. Int. J. Heat Mass Transf. **22**, 1461–1462 (1979)

Minkowycz, W.J., Cheng, P., Chang, C.H.: Mixed convection about a nonisothermal cylinder and sphere in a porous medium. Numer. Heat Transf. **8**, 349–359 (1985)

Nield, D.A., Kuznetsov, A.V.: The Cheng-Minkowycz problem for natural convective boundary layer flow in a porous medium saturated by a nanofluid. Int. J. Heat Mass Transf. **52**, 5792–5795 (2009a)

Nield, D.A., Kuznetsov, A.V.: Thermal instability in a porous medium layer saturated by a nanofluid. Int. J. Heat Mass Transf. **52**, 5796–5801 (2009b)

Pop, I., Ingham, D.B.: Natural convection about a heated sphere in a porous medium. In: Heat Transfer, vol. 2, pp. 567–572. Hemisphere, New York (1990)

Ranganathan, P., Viskanta, R.: Mixed convection boundary layer flow along a vertical surface in a porous medium. Numer. Heat Transf. **7**, 305–317 (1984)

Sano, T.: Unsteady forced and natural convection around a sphere immersed in a porous medium. J. Eng. Math. **30**, 515–525 (1996)

Yan, B., Pop, I., Ingham, D.B.: A numerical study of unsteady free convection from a sphere in a porous medium. Int. J. Heat Mass Transf. **40**, 893–903 (1997)